Available online at www.sciencedirect.com
ScienceDirect
International Journal of Heat and Mass Transfer 50 (2007) 2425–2433
International Journal of HEAT and MASS TRANSFER
www.elsevier.com/locate/ijhmt

Analysis of heat-aided membrane-controlled drug release from a process control perspective

Laurent Simon *

Otto H. York Department of Chemical Engineering, New Jersey Institute of Technology, Newark, NJ 07102, USA

Received 27 June 2006; received in revised form 12 August 2006
Available online 20 February 2007

Abstract

Analytical solutions were derived for the time lag and steady-state transdermal flux of drugs across a heat-aided drug-delivery device. The expressions incorporate thermodynamic and physical properties of the solvent/medicament and membrane system, making the approach amenable to *in silico* evaluation of process performance in a spreadsheet-like environment. Methods and concepts from classical control theory were applied to predict the onset of the steady-state flux. The methodology was based on the system's time constant, computed by taking the inverse of the first eigenvalue of a Sturm–Liouville problem. This framework does not require a solution to the transient heat-enhanced diffusion problem and relaxes the assumption of a constant diffusion coefficient throughout the membrane. The results match published data, partially explain some clinical trial observations, and suggest a novel method to control the plasma drug concentration. An optimal control strategy was proposed to keep the delivery rate as close as possible to 9.07 μg cm^{-2} h^{-1} over a 30-min period by adjusting the skin surface temperature. The integral of the absolute value of the error was 1138.19 compared to 1217.08 when the surface temperature was fixed at 37 °C.

Keywords: Heat-aided drug delivery; Membrane; Flux; Optimal control

1. Introduction

Because of drawbacks in drug-delivery methods, such as tablets, injections and sprays, new techniques are being explored that can ensure the delivery of a wide range of biomolecules while minimizing side effects. The use of transdermal patches for accurate delivery of medicaments to their target sites is one possible non-invasive technique. Entry into the systemic circulation through the skin circumvents first-pass metabolism and significantly decreases fluctuations in the blood concentration of a drug. Along with their cost effectiveness, these patches also offer great potential for enhanced patient compliance. The patch is painless, easy to apply, and remains in place for an extended period of time, during which a slow, controlled amount is released to the body. Patients receive the necessary medication without a disruption in lifestyle and day-to-day activities. Complex chemical enhancers are often added to the formulation to improve transdermal drug delivery by reducing the resistance of the stratum corneum to the drug molecules.

Some researchers have investigated the use of local heat to regulate transcutaneous drug absorption [1,2]. Systems, such as fentanyl patches – A narcotic opioid drug administered in the form of a transdermal patch to treat chronic pain – may take a long time to establish a steady-state blood level of medicament [1]. As a result, a short-acting medicament is often necessary to treat the breakthrough pain [2]. A heat-enhanced transdermal system may decrease the time it takes for the drug to reach a steady-state concentration in the blood, thereby eliminating the need to administer multiple injections.

The use of heat to enhance percutaneous absorption has received increased attention in recent years. However,

* Tel.: +1 973 596 5263; fax: +1 973 596 8436.
E-mail address: laurent.simon@njit.edu

0017-9310/$ - see front matter © 2007 Elsevier Ltd. All rights reserved.
doi:10.1016/j.ijheatmasstransfer.2007.01.001

predictive tools, which can help understand the effect of heat on the transdermal delivery of medicaments, are lacking in the literature. The purpose of this work is to use principles of transport phenomena, especially mass and heat transfer, and process control theory to gain a greater insight into the mechanism of heat-aided drug release and to improve this emerging technology. A firm understanding of fundamental principles behind this unique approach will help assess its relevance and efficiency and provide tools to facilitate the development of innovative drug-delivery systems. In this contribution, an expression of the rate of drug permeation, in terms of physicochemical parameters, is provided and tested using literature data. The time lag (t_{lag}) and the time to reach 98% of the steady-state membrane flux ($t_{0.98}$) are estimated. In addition, an optimal controller is developed to keep the transdermal flux as close as possible to a desired value.

2. Heat-aided membrane-controlled drug release model

Tojo et al. [3] studied drug transport through a polymeric membrane under nonisothermal conditions. They used a silicone (polydimethylsiloxane) membrane (0.013 cm thick) between the donor and receiver compartments (Fig. 1). The model drugs were testosterone and desoxycorticosterone in an aqueous 40% PEG solution. The mathematical models and main assumptions are reproduced here for completeness:

- The temperature gradient across the membrane does not cause drug transport. This conclusion implies that thermal diffusion (Soret effect) is not significant in the process.
- The drug concentration profile in the membrane can be represented by:

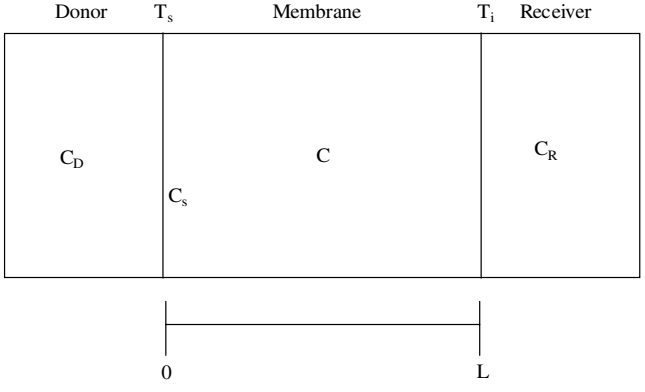

Fig. 1. Drug permeation across a membrane. Drug concentration in the membrane: C drug concentration at the donor/membrane interface: C_s; drug concentration in the donor chamber: C_D; drug concentration in the receiver chamber: C_R; temperature at the donor/membrane interface: T_s; temperature at the membrane/receiver interface: T_i; the membrane thickness: L.

$$\frac{\partial C}{\partial t} = \frac{\partial}{\partial x}\left(D[x]\frac{\partial C}{\partial x}\right) \tag{1}$$

where $D[x]$ is the drug diffusivity, which follows the Arrhenius relationship:

$$D[x] = D_0 e^{-\frac{E_d}{RT_0}\left(\frac{T_0}{T[x]}-1\right)} \tag{2}$$

where D_0 is the drug diffusivity at T_0 (310.15 K), R is the gas constant and E_d is the activation energy for diffusion through the polymer matrix (3).

The boundary conditions are:

$$C[L,t] = 0 \tag{3}$$

and

$$C[0,t] = C_{s0} e^{-\frac{E_s}{RT_0}\left(\frac{T_0}{T_s}-1\right)} \tag{4}$$

where E_s is the overall energy of solvation and partitioning and C_{s0} is the concentration at the donor/membrane interface at T_0. In Fig. 1, $C[L,t] = C_R = 0$.

The initial condition is:

$$C[x,0] = 0 \tag{5}$$

A linear profile is adequate to model the change of temperature in the membrane:

$$T[x] = ax + b \tag{6}$$

where a and b are parameters of the model.

This assumption is based on a steady-state heat transfer analysis (Fourier's Law):

$$\frac{q}{A} = -k\frac{dT}{dx} \tag{7}$$

stating that the time rate of heat flow q through a slab is proportional to the gradient of temperature difference. A is the transversal surface area, x is the length of the path measured perpendicular to A, k is the thermal conductivity of the substance. It should be noted that an analytical solution to the problem defined above, including the steady-state version, was not derived in the work of Tojo et al. [3]. They used the method of lines and tested the accuracy of the numerical scheme by comparing the results with those obtained from an isothermal system.

3. Prediction of the steady-state flux

The steady-state process is defined by:

$$\frac{d}{dx}\left(D[x]\frac{dC}{dx}\right) = 0 \tag{8}$$

with boundary conditions:

$$C[L] = 0 \tag{9}$$

and

$$C[0] = C_{s0} e^{-\frac{E_s}{RT_0}\left(\frac{T_0}{T_s}-1\right)} \tag{10}$$

with $D[x]$ defined by Eq. (2).

By taking into account the interfacial temperatures, Eq. (6) can be written as:

$$T[x] = \left(\frac{T_i - T_s}{L}\right)x + T_s \tag{11}$$

Using the substitution of variable:

$$V[x] = D[x]\frac{dC}{dx} \tag{12}$$

Eq. (8) becomes:

$$\frac{d}{dx}(V[x]) = 0 \tag{13}$$

or

$$V[x] = c_1 \tag{14}$$

Eq. (12) is integrated to yield:

$$C[x] = c_1 \int_0^x \frac{1}{D[\zeta]}d\zeta + c_2 \tag{15}$$

where c_1 and c_2 are integration constants.

The solution of the steady-state problem is obtained after applying the boundary conditions:

$$C[x] = -\frac{C[0]}{\int_0^L \frac{1}{D[x]}dx}\int_0^x \frac{1}{D[\zeta]}d\zeta + C[0] \tag{16}$$

or

$$C[x] = \frac{Q[x]}{P} \tag{17}$$

with

$$Q[x] = e^{\frac{E_s\left(\frac{1}{T_0}-\frac{1}{T_s}\right)}{R}}C_{s0} \times \left\{ \begin{array}{l} E_d L \times \left(Ei\left[\frac{E_d}{RT_i}\right] - Ei\left[\frac{E_d L}{R\times(xT_i+(L-x)T_s)}\right]\right) \\ -e^{\frac{E_d}{RT_i}}LRT_i + e^{\frac{E_d L}{R\times(xT_i+(L-x)T_s)}}R\times(xT_i+(L-x)T_s) \end{array} \right\} \tag{18}$$

and

$$P = L\left(E_d\left(Ei\left[\frac{E_d}{RT_i}\right] - Ei\left[\frac{E_d}{RT_s}\right]\right) - e^{\frac{E_d}{RT_i}}RT_i + e^{\frac{E_d}{RT_s}}RT_s\right) \tag{19}$$

where $Ei[\cdot]$ is the exponential integral function defined as:

$$Ei[z] = -\int_{-z}^{\infty}\frac{e^{-t}}{t}dt \tag{20}$$

Using the definition:

$$J = -D[L]\left(\frac{dC}{dx}\right)_{x=L} \tag{21}$$

and the relation:

$$\frac{dEi[z]}{dz} = \frac{e^z}{z} \tag{22}$$

we obtain

$$J = \frac{D_0 e^{\frac{\frac{E_d+E_s}{T_0}-\frac{E_s}{T_s}}{R}}RC_{s0}(T_s - T_i)}{L\left(E_d\left(Ei\left[\frac{E_d}{RT_i}\right] - Ei\left[\frac{E_d}{RT_s}\right]\right) - e^{\frac{E_d}{RT_i}} + e^{\frac{E_d}{RT_s}}RT_s\right)} \tag{23}$$

The integrations and subsequent symbolic computations were implemented in Mathematica®.

To estimate the concentration when $T_i = T_s$, we first notice that Eq. (17) takes an indeterminate form. L'Hospital rule is applied by taking the derivative of the numerator and denominator with respect to T_i. As a result, we have:

$$C[x] = \frac{C_{s0}e^{\frac{E_s(T_s-T_0)}{RT_0T_s}}(L-x)}{L} \tag{24}$$

Similarly, Eq. (23) becomes

$$J = \frac{C_{s0}D_0 e^{-\frac{(E_s+E_d)(T_0-T_s)}{RT_0T_s}}}{L} \tag{25}$$

Eqs. (24) and (25) are the widely used steady-state solutions for an isothermal system, in which materials are diffused through a plane sheet. The surfaces are maintained at constant concentrations specified by Eqs. (9) and (10). Eq. (23) is easily implemented using a spreadsheet. The exponential integral function is included in the program XNUMBERS 4.4 – Multi Precision Floating Point Computing and Numerical Methods for EXCEL [4].

4. Estimation of the time lag

The time lag estimates the onset of steady-state flux through a membrane. It has been used to predict the time elapsed from the point when a gas is brought into contact with a planar membrane until it exits the other side of the material at a constant rate (i.e., steady-state flux) [5]. In developing control drug-release systems, particular attention is paid to the time lag, in addition to the continuous delivery rate, to assure that patients receive the appropriate dosage in a relatively short time. For most systems, this important permeation parameter is computed by plotting the cumulative amount of drug released and extrapolating the steady-state portion of the plot to the time axis [6]. One of the limitations of this approach is that it assumes a constant diffusion coefficient throughout the membrane. The Frisch's technique, used in this work, is a more general method that relaxes the constant-diffusion coefficient assumption [5–8].

Eq. (1) is integrated from x to L:

$$\int_x^L \left(\frac{\partial C}{\partial t}\right)dy = \left[D[x]\frac{\partial C}{\partial x}\right]_x^L = D[L]\left(\frac{\partial C}{\partial x}\right)_{x=L} - D[x]\frac{\partial C}{\partial x} \tag{26}$$

As a result:

$$\int_x^L \left(\frac{\partial C}{\partial t}\right)dy = -J[t] - D[x]\frac{\partial C}{\partial x} \tag{27}$$

A spatial integration of Eq. (27) yields:

$$\int_0^L \left(\int_x^L \left(\frac{\partial C}{\partial t} \right) \mathrm{d}y \right) \mathrm{d}x = \int_0^L \left(-J[t] - D[x] \frac{\partial C}{\partial x} \right) \mathrm{d}x \tag{28}$$

or

$$\int_0^L \left(\int_x^L \left(\frac{\partial C}{\partial t} \right) \mathrm{d}y \right) \mathrm{d}x = -LJ[t] - \int_0^t \left(D[x] \frac{\partial C}{\partial x} \right) \mathrm{d}x \tag{29}$$

The integration of Eq. (29) in time gives:

$$\int_0^t \left\{ \int_0^L \left(\int_x^L \left(\frac{\partial C}{\partial t} \right) \mathrm{d}y \right) \mathrm{d}x \right\} \mathrm{d}t = \int_0^t \left(-LJ[t] - \int_0^L \left(D[x] \frac{\partial C}{\partial x} \right) \mathrm{d}x \right) \mathrm{d}t \tag{30}$$

which further simplifies to:

$$\int_0^L \left(\int_x^L (C[y,t]) \mathrm{d}y \right) \mathrm{d}x = -Lq[t] - \left(\int_0^L \left(D[x] \frac{\partial C}{\partial x} \right) \mathrm{d}x \right) t \tag{31}$$

after applying the initial condition given by Eq. (5). The cumulative amount transferred per unit area of membrane is $q[t] = \int_0^t J[t]\,\mathrm{d}t$ and its value can be obtained from Eq. (31):

$$q[t] = -\frac{\left(\int_0^L \left(D[x] \frac{\partial C}{\partial x} \right) \mathrm{d}x \right)}{L} \left\{ t + \frac{\int_0^L \left(\int_x^L (C[y,t]) \mathrm{d}y \right) \mathrm{d}x}{\left(\int_0^L \left(D[x] \frac{\partial C}{\partial x} \right) \mathrm{d}x \right)} \right\} \tag{32}$$

As $t \to \infty$, we have:

$$t_{\mathrm{lag}} = -\frac{\int_0^L \left(\int_x^L (C[y]) \mathrm{d}y \right) \mathrm{d}x}{\left(\int_0^L \left(D[x] \frac{\mathrm{d}C}{\mathrm{d}x} \right) \mathrm{d}x \right)} \tag{33}$$

where $C[x]$ is defined by Eqs. (16) or (24). For the isothermal case, Eq. (33) simplifies to:

$$t_{\mathrm{lag}} = -\frac{\int_0^L \left(\int_x^L C[y] \mathrm{d}y \right) \mathrm{d}x}{D_{\mathrm{c}} \left(\int_0^L \left(\frac{\mathrm{d}C}{\mathrm{d}x} \right) \mathrm{d}x \right)} = -\frac{\frac{1}{6} L^2 C_{\mathrm{s0}} \mathrm{e}^{\frac{E_{\mathrm{S}}(T-T_0)}{RTT_0}}}{D_{\mathrm{c}} \left(-C_{\mathrm{s0}} \mathrm{e}^{\frac{E_{\mathrm{S}}(T-T_0)}{RTT_0}} \right)} = \frac{L^2}{6D_{\mathrm{c}}} \tag{34}$$

where D_{c}, the diffusion coefficient obtained from Eq. (2), is independent of x as the temperature does not change across the membrane.

5. Prediction of the time required to reach 98% of the steady-state flux

A concept from classical control theory was applied to estimate the onset of steady-state flux: after four time constants, the response of a first-order process has essentially reached its ultimate value [9]. Furthermore, if a system $Y[s]$ is described by N first-order stable processes G_i in series, with poles s_i, such that a single dominant pole s_n exists, the time constant of the process can be approximated by the dynamic behavior of G_n. The system is represented by:

$$Y[s] = \frac{a_0}{s} + \sum_{i=1}^{N} \left(\frac{a_i}{\tau_{\mathrm{p}i} s + 1} \right) \tag{35}$$

where s is the Laplace variable; a_i and $\tau_{\mathrm{p}i}$ are the steady-state gain and time constant of the process, respectively. If the series is ordered so that the process with the dominant pole is $G_1 = \frac{a_1}{\tau_{\mathrm{p}1} s + 1}$, we have $s_1 = -\frac{1}{\tau_{\mathrm{p}1}}$. As a result, $t_{\mathrm{ss}} \sim= 4\tau_{\mathrm{p}1}$. The time response is obtained by taking the inverse Laplace transform of Eq. (35):

$$y[t] = a_0 + \sum_{i=1}^{N} \left(a_i \mathrm{e}^{-\frac{1}{\tau_{\mathrm{p}i}} t} \right) \tag{36}$$

In order to apply these definitions and concepts to the heat-enhanced membrane transport problem, it is critical to establish that the flux can be expressed in a form similar to Eq. (36).

First, the system defined by Eqs. (1)–(5) is transformed into a homogeneous boundary problem by using deviation variables:

$$\xi[x,t] = C[x,t] - C_{\mathrm{eq}}[x] \tag{37}$$

where $C_{\mathrm{eq}}[x]$ is the steady-state concentration defined by Eqs. (13) or (20). The transient problem becomes:

$$\frac{\partial \xi}{\partial t} = \frac{\partial}{\partial x} \left(D[x] \frac{\partial \xi}{\partial x} \right) \tag{38}$$

with homogeneous boundary conditions:

$$\xi[0,t] = 0 \tag{39}$$

and

$$\xi[L,t] = 0 \tag{40}$$

The initial condition becomes:

$$\xi[x,0] = -C_{\mathrm{eq}}[x] \tag{41}$$

We then use the method of separation of variables to obtain a solution to Eqs. (38)–(41):

$$\xi[x,t] = \sum_{i=1}^{\infty} (A_i \mathrm{e}^{-\lambda_i t}) \eta_i[x] \tag{42}$$

and

$$C[x,t] = C_{\mathrm{eq}}[x] + \sum_{i=1}^{\infty} (A_i \mathrm{e}^{-\lambda_i t}) \eta_i[x] \tag{43}$$

where the Fourier coefficients A_i are determined by applying the initial condition (Eq. (5)) and using the orthogonality of the eigenfunctions $\eta_i[x]$. The eigenvalues are defined by λ_i. Furthermore, the eigenmodes satisfy:

$$-\frac{\mathrm{d}}{\mathrm{d}x} \left(D[x] \frac{\mathrm{d}\eta_i[x]}{\mathrm{d}x} \right) = \lambda_i \eta_i[x] \tag{44}$$

with boundary conditions:

$$\eta_i[0] = 0 \tag{45}$$

and

$$\eta_i[L] = 0 \tag{46}$$

The rate of drug permeation takes the form of Eq. (36):

$$J = J_{ss} + \sum_{i=1}^{\infty}(B_i e^{-\lambda_i t}) \tag{47}$$

with

$$B_i = D[L]A_i\left(\frac{d\eta_i[x]}{dx}\right)_{x=L} \tag{48}$$

Several methods, including piecewise constant perturbation methods, can be used to compute the eigenvalues without fully solving the transient problem [10]. There are an infinite number of eigenvalues labeled $\lambda_1, \lambda_2, \ldots$ so that $\lambda_n < \lambda_m$ if $n < m$. The dominant eigenvalue λ_1 estimates the time it takes to reach the steady-state flux. In this case, $\tau_{p1} = \frac{1}{\lambda_1}$ and the time required to reach the steady-state flux is $4\tau_{p1}$. The software MATSLISE [10] was used to compute λ_1.

6. Results and discussion

6.1. Estimation of the steady-state flux

Membrane, solvent, and drug properties were evaluated in order to compare predicted and experimental J_{ss} values. Tojo et al. [3] considered the presence of thermal boundary layers and estimated their thickness based on correlation equations developed for hydrodynamic boundary layers [11–13]. These results, in addition to thermal conductivity values, helped to compute the surface temperatures. They also provided thermodynamics and physical properties for the solvent, 40% PEG 400 solution, and the silicone membrane used in their experiments. Missing from their report were the density (ρ) and the viscosity (μ) of the solvent at the temperatures investigated. These properties were necessary to compute the thickness of the layers in the donor (l_d) and receiver (l_r) chambers [3]:

$$\frac{d}{l_i} = 0.234\left(\frac{Nd^2\rho}{\mu}\right)^{0.57}\left(\frac{C_p\mu}{k}\right)^{0.33} \tag{49}$$

where d represents the length of the magnetic stirrer; N is the rotational speed of the stirrer, l_i is the thickness of the boundary layer in the donor (i = d) or receiver chamber (i = r); C_p is the heat capacity; k is the thermal conductivity. In this contribution, ρ and μ values were estimated using correlations described in [13–15] and Andrade's viscosity equation:

$$\ln[\mu] = a_0 + \frac{a_1}{T} \tag{50}$$

where a_0 and a_1 are constant and T is the temperature (K).

The results are listed in Tables 1 and 2 for testosterone and desoxycorticosterone, respectively. The predicted fluxes are in close agreement with the experimental values. Deviations, such as the ones observed at $T_d = 17$ and 27 °C, may be due to errors in the estimated diffusion coefficient of desoxycorticosterone at 37 °C (D_0 in Eq. (2)). Although prepared under similar production conditions as the other ones (Batch 1), the membranes, employed in the desoxycorticosterone permeation studies at $T_d = 17$, 27, and 47 °C, were obtained from a different batch (Batch 2) [3]. Another experiment, conducted at $T_d = 37$ °C (not shown in Table 2), yielded a flux of 21.8 μg cm^{-2} h^{-1} for Batch 2, compared to 18.0 μg cm^{-2} h^{-1} in the case of Batch 1. This may explain the relatively low J_{ss} values estimated at $T_d = 17$, 27, and 47 °C.

Tojo et al. (1987), in studying drug transport under non-isothermal conditions, varied the donor temperature from 10 °C to 60 °C to simulate realistic environmental conditions while the receptor solution was kept at 37 °C (in most cases) [3]. As a result, positive and negative temperature gradients were generated across the membrane. Akomeah et al. (2004) investigated the effect of heat on the delivery of three model penetrants (i.e., methyl paraben, butyl paraben, and caffeine) through artificial membranes and human epidermis [16]. Positive temperature gradients were used: 22–23 °C in the donor cell and a range of 23–45 °C in the receptor compartment. They also observed an increase in the steady-state flux when the temperature rose. Clinical studies showed that the plasma level of nitroglycerin increased from 3.1 to 7.6 nmol l^{-1} after 10 min of heating (250 W heating bulb) and decreased from 2.1 to 1.4 nmol l^{-1} after 15 min of cooling (ice cubes) [17] the patch application area.

Table 1
Steady-state flux of testosterone at different surface temperatures

T_d/°C	l_d/m	T_r/°C	l_r/m	T_s/°C	T_i/°C	J_{ss}/μg cm^{-2} h^{-1}	J^*_{ss}/μg cm^{-2} h^{-1}	λ_1/s^{-1}	λ_2/s^{-1}	τ_p/s	$t_{0.98}$/s	$J_{ss}/J[\tau_p]$/%	t_{lag}/s
10	0.000734	10	0.000734	10.00	10.00	0.93	0.98	0.0039	0.0156	256.59	1026.34	96.14	422.07
20	0.000681	20	0.000681	20.00	20.00	2.28	2.04	0.0061	0.0244	163.74	654.95	96.19	269.34
37	0.000615	37	0.000615	37.00	37.00	9.07	8.83	0.0123	0.0491	81.54	326.16	96.30	134.13
50	0.000566	50	0.000566	50.00	50.00	23.68	22.19	0.0199	0.0796	50.27	201.09	96.35	82.69
50	0.000566	37	0.000615	44.73	42.27	15.48	18.62	0.0157	0.0628	63.71	254.86	96.26	107.25
10	0.000734	37	0.000615	21.44	25.56	2.81	4.21	0.0071	0.0284	140.97	563.89	96.19	222.08
20	0.000681	37	0.000615	27.12	29.88	4.38	5.22	0.0087	0.0349	114.44	457.74	96.22	183.02
30	0.000640	37	0.000615	32.90	34.10	6.75	6.73	0.0107	0.0428	93.53	374.14	96.23	152.04

Temperature at the donor/membrane interface: T_s; temperature at the membrane/receiver interface: T_i; thickness of thermal boundary layer in the donor chamber: l_d; thickness of thermal boundary layer in the receiver chamber: l_r; predicted and experimental steady-state flux: J_{ss} and J^*_{ss}, respectively.

Table 2
Steady-state flux of desoxycorticosterone at different surface temperatures

T_d/°C	l_d/m	T_r/°C	l_r/m	T_s/°C	T_i/°C	J_{ss}/μg cm^{-2} h^{-1}	J^*_{ss}/μg cm^{-2} h^{-1}	λ_1/s^{-1}	λ_2/s^{-1}	τ_p/s	$t_{0.98}$/s	$J_{ss}/J[\tau_p]$/%	t_{lag}/s
17	0.000697	37	0.000615	25.40	28.60	7.73	13.2	0.0125	0.0498	80.32	321.27	96.23	128.83
27	0.000651	37	0.000615	31.16	32.84	11.36	17.3	0.0146	0.0582	68.69	274.76	96.24	111.54
30	0.000640	37	0.000615	32.90	34.10	12.73	14.8	0.0152	0.0610	65.61	262.43	96.25	106.94
37	0.000615	37	0.000615	37.00	37.00	16.54	18.0	0.0169	0.0677	59.05	236.18	96.32	97.13
47	0.000576	37	0.000615	42.93	41.07	23.84	25.6	0.0196	0.0784	51.01	204.02	96.29	85.04
50	0.000566	37	0.000615	44.73	42.27	26.55	24.7	0.0205	0.0819	48.86	195.43	96.27	81.80
60	0.000537	37	0.000615	50.77	46.23	37.77	38.1	0.0236	0.0942	42.46	169.84	96.33	72.09

Temperature at the donor/membrane interface: T_s; temperature at the membrane/receiver interface: T_i; thickness of thermal boundary layer in the donor chamber: l_d; thickness of thermal boundary layer in the receiver chamber: l_r; predicted and published steady-state flux: J_{ss} and J^*_{ss}, respectively.

Maintaining a positive or negative temperature gradient across the membrane influences the diffusion coefficient (Eqs. (2) and (6)) and therefore the drug-delivery rate through the membrane. It is worth noticing that, in the case of desoxycorticosterone and a receptor compartment temperature of 37 °C, the predicted steady-state flux increased from 16.54 to 23.84 μg cm^{-2} h^{-1} ($\Delta J_{ss} = 7.30$ μ cm^{-2} h^{-1}) when the donor cell temperature changed from 37 to 47 °C ($\Delta T = 0$ to -10 °C, $\Delta T = T_r - T_d$). The increase ($\Delta J_{ss} = 5.18$ μg/cm^{-2} h^{-1}) was less significant when T_d changed from 27 to 37 °C. Computation of an average diffusion coefficient D_{ave} may help explain those differences. Using the equation $D_{ave} = \int_0^L D[x]\,dx / \int_0^L x\,dx$, the D_{ave} values for $T_r = 37$ °C and T_d set at 27, 37, and 47 °C are 2.49×10^{-11}, 2.90×10^{-1} and 3.36×10^{-11} m^2/s, respectively. Consequently, the sign of the temperature gradient affects the transdermal flux by altering the average drug diffusion coefficient in the membrane. The magnitude of the response is a function of the activation energy for diffusion. Since the process is also driven by the concentration difference across the membrane, the increase in $C[0]$ (i.e., solubility effect) by changing T_d from 27 to 47 °C is also a factor for consideration: when T_d is set at 27, 37, and 47 °C, $C[0] = 0.165$, 0.206, and 0.256 kg/m^3, respectively.

6.2. Prediction of t_{lag} and $t_{0.98}$

The time lags, corresponding to the release of testosterone and desoxycorticosterone under several experimental conditions, were computed using Eqs. (33) and (34) (Tables 1 and 2). After solving the transient problem, numerically, using the method of lines (*Mathematica*, Wolfram, Inc), the flux profiles were plotted for testosterone and desoxycorticosterone (Figs. 2 and 3, respectively). The first two eigenvalues were estimated using the *Matlab* package (Mathworks, Inc.), MATSLISE [10]. Although the second eigenvalue is not needed to calculate $t_{0.98}$, it is listed to show that λ_1 was significantly smaller than λ_2 (Tables 1 and 2). As illustrated by the location of the filled circle (x-coordinate: $4\tau_{p1}$; y-coordinate: $J[4\tau_{p1}]$) on the flux profiles, it is clear that the dominant eigenvalue method can be used to estimate $t_{0.98}$.

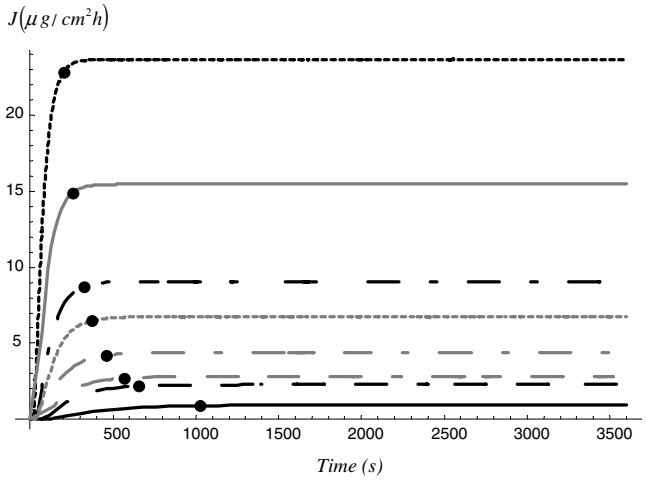

Fig. 2. Permeation flux profiles of testosterone. The x-coordinate of the filled circle is $4\tau_{p1}$. The lines represent the flux profiles of testosterone using the conditions specified in entries 1–8, respectively (Table 1):

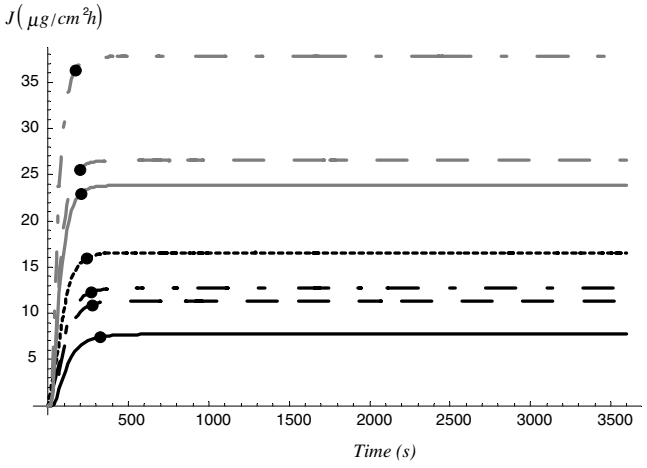

Fig. 3. Permeation flux profiles of desoxycorticosterone. The x-coordinate of the filled circle is $4\tau_{p1}$. The lines represent the flux profiles of desoxycorticosterone using the conditions specified in entries 1–7, respectively (Table 2):

The dominant pole analysis suggests a simple method of estimating the time-varying drug-release rate to the receiver. Since the drug concentration in the membrane can be written as $C[x,t] = C_{eq}[x](1 - e^{-\lambda_1 t})$, it follows that the transient flux takes the form $J(t) = -D[L](1 - e^{-\lambda_1 t})\left(\frac{dC_{eq}[x]}{dx}\right)_{x=L}$. In cases where the steady-state concentration $C_{eq}[x]$ varies linearly across the membrane, a quick experimental determination of t_{ss}, and therefore λ_1 (since $\lambda_1 \approx 4/t_{ss}$), should allow the evaluation of $J(t)$.

Results obtained in this study are in agreement with clinical trial observations. The use of controlled heat was found to aid the delivery of testosterone through the membrane by increasing the maximum serum drug levels by 48% and by reducing the time-to-peak serum testosterone concentration [18]. Although it would be necessary to add to the transient system described in this work an unsteady mass-balance equation, which includes the flux, the accumulation and the elimination rates of the drug in the plasma, the findings of Shomaker et al. [18] can be partially explained in light of this contribution. Using a single-compartment model to describe the plasma drug concentration profile:

$$\frac{dC_p}{dt} = \frac{A}{V}J - k_{te}C_p \tag{51}$$

it can be shown that, if other factors remain constant, a higher J_{ss} value would be accompanied by an increase in the mean maximum serum testosterone concentration. In Eq. (51), V is the apparent distribution volume; C_p is the plasma drug concentration, k_{te} is a first-order elimination rate constant. Also, for the same temperature in the receiver chamber, λ_1 increases with T_d. Consequently, the steady-state flux is reached in a shorter period, thereby decreasing the time-to-peak serum drug concentration. This analysis assumes that λ_1 is much less than $\frac{1}{k_{te}}$.

This work may also explain the findings of Shomaker et al. [19]. Based on a study conducted of six healthy adult volunteers, they concluded that local heat can decrease the time it takes fentanyl to reach a steady-state concentration when the Fentanyl Transdermal Drug Delivery System™ (TFDS) (TSS-Fentanyl, Alza Corp., Palo Alto, CA) is used [19]. Akomeah and co-workers [16] also reported that an increase in the temperature of the receiver, in an *in-vitro* study, enhanced the transdermal permeation of methyl paraben, butyl paraben and caffeine. This trend can be predicted using the results summarized in Table 1. In addition, the onset of steady-state flux can be estimated using t_{lag} or $t_{0.98}$. The new parameter, $t_{0.98}$, may be used in conjunction with the conventional t_{lag} to provide additional information about the transient behavior of the system. From a process control perspective, the introduction of eigenvalues in the analysis of heat-aided transdermal drug-delivery processes offers the opportunity to set dynamic response performance criteria that would facilitate the timely release of a drug molecule.

Mathematically inspired schemes, such as the one described in this contribution, have been applied successfully in other fields. Computational analytical methods have helped to minimize chances of allograft rejection and toxicity in organ transplantation [20] and have inspired the use of pulse vaccination strategies as opposed to constant rates of vaccine administration [21]. Based on the promises and advantages of these methods, more effort should be devoted to model-based optimization in transdermal drug-delivery research [22]. Preliminary clinical studies have demonstrated that the use of heat in the transdermal delivery of drugs, such as fentanyl and testosterone, has increased the maximum serum concentration and shortened the time to achieve a therapeutic effect. These findings suggest that the applied temperature (i.e., the heat transferred) could be used as a manipulated variable to control the plasma drug concentration.

Some practical issues need to be addressed before using the results to predict transdermal drug absorption. Increasing the flux rate using a heat-aided device takes place in two steps. First, the diffusion of the drug through the drug reservoir/rate-controlling membrane is altered. Second, the permeation properties of the skin and/or the blood flow to the area are modified. The present work solely focuses on the mechanism of transport through a membrane. The model does not discuss issues related to the maximum enhancement of flux, toxicity/stability limit, and heat protection provided by the system. These factors limit the applicability of the system to fully explain clinical data on heat-enhanced transdermal uptake of drugs. The model can, however, be used to suggest a method of optimizing the drug-delivery rate by modulation of the skin surface temperature.

6.3. Optimal control of the drug-delivery rate

With a preset T_i, a specified delivery rate can be obtained by setting the skin surface temperature to an appropriate value (Tables 1 and 2). The T_s value can be estimated by performing a number of experiments or by solving Eq. (23). It is important to note that, in either case, the time to reach the steady-state flux is also fixed, a conclusion supported by the computation of t_{lag} or $t_{0.98}$. An often-desired outcome, not addressed in the current analysis, is the drug-delivery rate reaching a user-defined value in a very short period of time and with minimum overshoot. This approach is significant to drug-release device manufacturers and clinicians who are interested in combining a reduced number of clinical trials with simulation data to predict individual pharmacokinetics and to recommend drug-dosage regimens. Dynamic programming techniques can assist in the development of these regimens.

Dynamic programming techniques consist of determining control and state histories for a dynamic system over a finite time period to minimize a performance index [23]. The method has been used to optimize treatment strategies within a very short time frame and at a relatively low cost. Dose optimization is usually carried out using compartmental models represented by a system of ordinary

differential equations (ODEs). One optional form for the optimal drug administration is:

$$\underset{D_0,\ldots,D_m,t_0,\ldots,t_m}{\text{Min}} \int_0^{t_f} |x(t) - x_{\text{set}}|\,dt \tag{52}$$

(i.e., the integral of the absolute value of the error) where D_i is a dose given at time t_i; $x(t)$ is the concentration of the drug in an organ at time $t > 0$; x_{set} is the desired value of x. Constraints, such as the maximum allowed concentration, dosage, and drug exposure are easily added. In this work, the target is the drug-delivery rate. Eq. (52) is modified by replacing the dose, D_i, with T_s, the temperature applied to the skin. A constant time interval is specified to simplify the problem:

$$\underset{T_{s0},\ldots,T_{s}m}{\text{Min}} \int_0^{t_f} |J(t) - J_{\text{set}}|\,dt \tag{53}$$

The temperature is constrained between T_{s0} and T_{sm}. The solution to Eq. (53) is a set of mT_s values implemented from time 0 to t_f such that $J(t)$ remains as close as possible to J_{set}. To implement the optimal control problem, the original PDE is first converted to a system of ODEs using orthogonal collocation techniques [24,25]. Four internal collocation points were sufficient to capture the process dynamics. The procedure was tested using the silicone/testosterone system at $T_i = 37$ °C and a desired flux of 9.07 μg cm^{-2} h^{-1} (Table 1). Since a surface temperature of 37 °C was necessary to achieve the target, it was of special interest to compare the result with an optimal sequence of T_s values, implemented at equal time intervals ($\Delta t =$ 7.5 min, $t_f = 30$ min) under the constraint $10\,^{\circ}\text{C} \leqslant T_s \leqslant 50\,^{\circ}\text{C}$ (i.e., lowest and highest surface temperatures investigated in [3]). The results are shown in Fig. 4. The optimal T_s values are: 37.63, 36.98, 37.00, 37.00 °C. The IAE for the optimal drug administration is 1138.19 compared to 1217.08 hen the surface temperature is kept at 37 °C. The dynamic programming approach results in a faster rise time and minimum error at the expense of a slight overshoot in the target flux. It should be noted that the solution is affected by the performance criterion and the number of collocation points. The benefit of reaching the desired delivery rate as soon as possible with the downside of overshooting the target should be weighed before implementation.

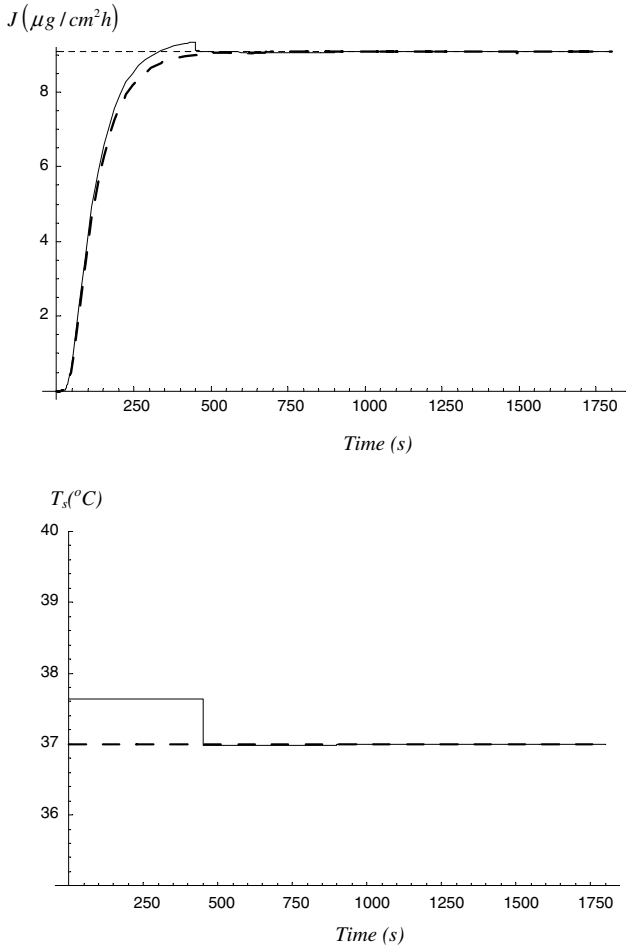

Fig. 4. Optimal permeation flux profile of testosterone. The transdermal flux ▬ ▬ is the response when the skin temperature T_s ▬ ▬ is kept at 37 °C. The solid lines (—) represent the optimal solution and the resulted flux. The target flux (9.07 μg cm^{-2} h^{-1}) is represented by ----.

7. Conclusions

A closed-form solution for the steady-state flux of drugs across a heat-aided drug-delivery device was developed and tested using published data on the *in vitro* delivery of testosterone and desoxycorticosterone. In the cited report, the apparatus consisted of a 40% PEG 400 solution in the donor and receiver compartments and a silicone membrane mounted between the cells. For a constant temperature in the receiver, the flux increases with the temperature in the donor chamber. The steady-state flux and time lag expressions incorporate properties, such as the drug diffusion coefficient, the energy of solvation and partitioning and the activation energy for diffusion. Consequently, clinicians can easily evaluate the effects of a host of environmental conditions on the performance of a new device by conducting *in silico* experiments. The time it takes to reach 98% of the steady-state flux was estimated by multiplying by four the inverse of the first eigenvalue of a Sturm–Liouville problem. The results were validated by numerically solving the transient problem and locating the onset of steady-state flux. These findings promote a novel strategy to control the plasma drug concentration by modulation of the skin's surface temperature. Using a time-integral performance criterion, it was possible to design a controller that reduced the rise time to reach the steady-state flux.

References

[1] M.A. Ashburn, L.L. Ogden, J. Zhang, G. Love, S.V. Basta, The pharmacokinetics of transdermal fentanyl delivered with and without controlled heat, J. Pain 4 (2003) 291–297.

[2] K.A. Carter, Heat-associated increase in transdermal fentanyl absorption, Am. J. Health Syst. Pharm. 60 (2003) 191–192.
[3] K. Tojo, Y.W. Chien, Y. Sun, M. Ghannam, Membrane transport of drug under nonisothermal conditions, J. Chem. Eng. Jpn. 20 (1987) 626–629.
[4] Foxes Team, Reference for X.NUMBERS.XLA – Numeric Calculus in Excel, Italy, 2005.
[5] H.L. Frisch, Time lag in diffusion, J. Phys. Chem. 61 (1957) 93–95.
[6] J. Crank, The Mathematics of Diffusion, second ed., Oxford University Press Inc, New York, 1975.
[7] R.A. Siegel, E.L. Cussler, Reactive barrier membranes: some theoretical observations regarding the time lag and breakthrough curves, J. Membr. Sci. 229 (2004) 33–41.
[8] R.A. Siegel, Characterization of relaxation to steady state in membranes with binding and reaction, J. Membr. Sci. 251 (2005) 91–99.
[9] G. Stephanopoulos, Chemical Engineering Control. An Introduction to Theory and Practice, PTR Prentice Hall, Englewood Cliffs, 1984.
[10] V. Ledoux, M.V. Daele, G.V. Berghe, MATSLISE: A MATLAB package for the numerical solution of Sturm–Liouville and Schrodinger, ACM Trans. Math. Softw. 31 (2005) 532–554.
[11] K. Tojo, Y. Sun, M.M. Ghannam, Y.W. Chien, Characterization of a membrane permeation system for controlled drug delivery studies, AlChE J. 31 (1985) 741–746.
[12] K. Tojo, M. Ghannam, Y. Sun, Y.W. Chien, In vitro apparatus for controlled release studies and intrinsic rate of permeation, J. Contr. Release 1 (1985) 197–203.
[13] W.L. McCabe, J.C. Smith, P. Harriot, Unit Operations of Chemical Engineering, fifth 5th ed., McGraw-Hill Inc., New York, 1993.
[14] L. Ninni, H. Burd, W.H. Fung, A.J.A. Meirelles, Kinematic viscosities of poly(ethylene glycol) aqueous solutions, J. Chem. Eng. Data 48 (2003) 324–329.
[15] C.J. Geankoplis, Transport Processes and Separation Process Principles, fourth ed., Prenctice Hall, Engelwood, 2003.
[16] F. Akomeah, T. Nazir, G.P. Martin, M.B. Brown, Effect of heat on the percutaneous absorption and skin retention of three model penetrants, Eur. J. Pharm. Sci. 21 (2004) 337–345.
[17] T.O. Klemsdal, K. Gjesdal, J.-E. Bredesen, Heating and cooling of the nitroglycerin patch application area modify the plasma level of nitroglycerin, Eur. J. Clin. Pharmacol. 43 (1992) 625–628.
[18] T.S. Shomaker, J. Zhang, M.A. Ashburn, A pilot study assessing the impact of heat on the transdermal delivery of testosterone, J. Clin. Pharmacol. 41 (2001) 677–682.
[19] T.S. Shomaker, J. Zhang, M.A. Ashburn, Assessing the impact of heat on the systemic delivery of fentanyl through the transdermal fentanyl delivery system, Pain Med. 1 (2000) 225–230.
[20] A. Ruggeri, M. Martinelli, A program for the optimization of cyclosporine therapy using population kinetics modeling, Comput. Meth. Progr. Biomed. 61 (2000) 61–69.
[21] B.V. Shulgin, L. Stone, Z. Agur, Theoretical examination of pulse vaccination in the SIR epidemic model, Math. Comput. Model. 31 (2000) 207–215.
[22] L. Simon, M. Fernandes, Neural network-based prediction and optimization of estradiol release from ethylene-vinyl acetate membranes, Comput. Chem. Eng. 28 (2004) 2407–2419.
[23] A.E. Bryson, Dynamic Optimization, Addison-Wesley, Berkeley, 1999.
[24] B.A. Finlayson, Nonlinear Analysis in Chemical Engineering, MacGraw-Hill Book Company, New York, 1981.
[25] L. Simon, Observing biomass concentration in a fixed-bed bioreactor, Chem. Eng. Commun. 192 (2005) 272–285.